Numerical Methods for Nonreacting and Chemically Reacting Laminar Flows—Tests and Comparisons

CLARK H. LEWIS*
Virginia Polytechnic Institute and State University, Blacksburg, Va.

Equilibrium, nonequilibrium, and ideal gas ($\gamma = 1.4$) laminar boundary layers and viscous shock layers over a 10°-half-angle hyperboloid, 50 nose-radii long, have been computed by several investigators for three 20,000-fps cases, one at 100,000 ft altitude and two at 250,000 ft. Their predictions of skin-friction and heat-transfer coefficients and displacement-thickness distributions over the body, as well as property profiles across the layer at the ends of the body, are compared. The conditions were chosen to test the ability of the numerical methods to predict nonequilibrium viscous-layer flows near and far from chemical equilibrium and the applicability of boundary-layer theory at low-Reynolds-number conditions. Results show that recently developed finite-difference methods can be used to compute finite rate, chemically reacting flows near chemical equilibrium, and iterations of implicit finite-difference solutions are required for accurate results. At 250,000 ft altitude, higher-order boundary-layer theory is not adequate and a fully viscous shock-layer technique must be used. At the higher altitude, stagnation heat transfer is strongly affected by shock slip.

Nomenclature

$C_{f\infty}$	= $2\tau_w/\rho_\infty U_\infty^2$, skin-friction coefficient
C_i	= species mass fraction, g/g-mixture or moles/g-mixture
H	= stagnation enthalpy
M	= Mach number
p	= static pressure
P_T	= local Pitot pressure through the shock layer
q	= heat-transfer rate, Btu/ft²-sec
r	= radial distance normal to the axis
r_n	= body nose radius
Re_∞	= $\rho_\infty U_\infty/\mu_\infty$, freestream unit Reynolds number
s	= surface distance from forward stagnation point
St_∞	= $q_w/\rho_\infty U_\infty(H_\infty - H_w)$, Stanton number
T	= temperature
u	= tangential velocity component
U_∞	= freestream velocity
γ	= ratio of specific heats
δ^*	= boundary-layer displacement thickness
ρ	= mass density
$(\ )_0'$	= freestream normal shock stagnation conditions
BL	= boundary layer
ECW	= equilibrium catalytic wall with species diffusion and convection
EQ	= chemical equilibrium gas
MOC	= method of characteristics
NCW	= noncatalytic wall
NEQ	= finite-rate chemical nonequilibrium
SL	= viscous shock layer
SLSS	= shock layer with shock slip
TVSL	= thin viscous shock layer
TVSLSS	= thin viscous shock layer with shock slip

Subscripts

w, ∞ = wall and freestream, respectively

Introduction

A NUMBER of numerical methods have been developed for the solution of laminar boundary-layer flows of nonreacting and chemically reacting gases over two-dimensional and axisymmetric bodies at zero lift. In 1967 the Advisory Group for Aerospace Research and Development (AGARD) of the North Atlantic Treaty Organization sponsored a seminar on numerical methods in viscous flows at the National Physical Laboratory in Teddington, England. One objective was to compare results for selected cases, to test boundary-layer theory, computational methods, and chemical models used by various investigators. Preliminary results were given then; however, subsequent extensions and improvements now permit comparisons from more complete calculations.

This paper presents the results from those involved in the AGARD seminar for the specific set of test cases, including higher-order boundary-layer effects and the effects of various chemical models on measurable quantities. It is also hoped that other investigators who have developed operational methods will use these results for further tests and comparisons.

The results presented in this paper should be of interest to those concerned with entry vehicle design. Because of the cost of the numerical calculations, a wider range of conditions was not feasible. Of course, the few conditions chosen do not adequately test laminar boundary-layer theory with regard to either chemical effects or higher-order boundary-layer effects, and one should keep these points in mind when considering the results.

A recent AGARDograph,[1] contains papers describing in detail the flow models and numerical methods used for the calculations presented herein. In addition, it contains survey papers on higher-order boundary-layer theory by M. Van Dyke and chemically reacting laminar boundary-layer theory by F. G. Blottner.

Test Case Conditions

It is not possible to include here all data which were furnished to the various investigators, but from what is presented, it is possible to interpret the results presented and to perform nonreacting (perfect gas) laminar boundary-layer calculations.

Three test Cases A, B, and C, all for $U_\infty = 20{,}000$ fps, (Table 1). Case A at 100,000 ft altitude was specified to test finite-rate, chemically reacting flow models at conditions near chemical equilibrium. Cases B and C at 250,000 ft altitude are for reacting and perfect-gas ($\gamma = 1.4$) conditions, respectively. Case C also is used to explore higher-order

Received June 1, 1970; revision received October 26, 1970.
* Professor of Aerospace Engineering. Associate Fellow AIAA.

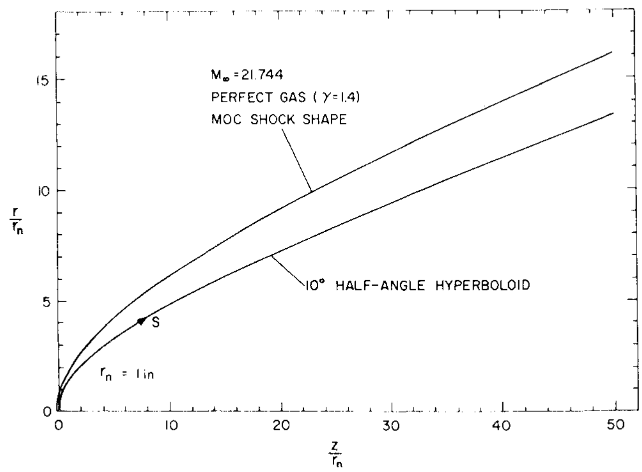

Fig. 1 Hyperboloid geometry and perfect-gas shock wave.

boundary-layer effects, since no method had been developed to treat such effects simultaneously with nonequilibrium effects.

The body, a 10° half-angle hyperboloid with a nose radius r_n of 1 in. and a length of 50 r_n is shown in Fig. 1. A comparison was made between modified Newtonian pressure distribution and the results of a blunt-body and characteristics solution for perfect gas flows over this shape. It was found that the differences in pressure distribution were negligible (5%); therefore, Newtonian pressure distribution was prescribed for all test conditions. For the chemically reacting viscous flow Cases A and B, frozen, equilibrium, and nonequilibrium streamtube expansions were performed from the equilibrium stagnation conditions given in Table 1 and for the Newtonian pressure distribution along the body using the method of Lordi and Mates.[2] Complete tabulations of these inviscid expansion data were provided to each of the investigators, and these data can be provided to others interested in making comparisons with the data presented in this paper by writing to the author of the present paper. Figure 2 shows the normalized temperature (T/T_0') and oxygen-concentration (C_{O_2}) distributions from the inviscid streamtube expansion data. The T/T_0' distribution for Case A (the nonequilibrium curve) is indeed near chemical equilibrium, whereas for Case B it is near the chemically frozen limit. However, C_{O_2} from the nonequilibrium expansions diverges rapidly downward relative to both the

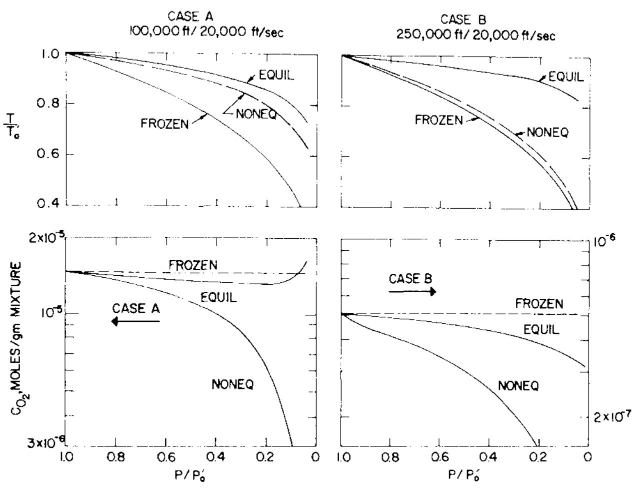

Fig. 2 Distributions of temperature and oxygen concentration from the inviscid streamtube expansions.

Table 1 Test case conditions

Case	A	B	C
Altitude, ft	100 K	250 K	250 K
Velocity, fps	20,000	20,000	20,000
M_∞	20.178	21.744	21.744
T_∞, °K	226.98	195.46	195.46
p_∞, atm	1.0997^{-2}	2.0074^{-5}	2.0074^{-5}
Re_∞/ft	2157943.	5192.	5192.
T_w, °K	1400	1000	1000
p_0', atm	6.0352[a]	0.0129[a]	0.01223[b]
T_0' °K	6996[a]	5302[a]	18,678[b]

[a] Equilibrium normal shock stagnation conditions.
[b] Ideal gas (γ = 1.4) normal shock stagnation conditions.

equilibrium and frozen limits for both cases. Therefore, it is desirable to use the complete set of nonequilibrium expansion data to determine the inviscid outer boundary-layer conditions, as Blottner[4] had noted.

The investigators were J. C. Adams, ARO Inc.; F. G. Blottner, Sandia Corporation; R. T. Davis, Virginia Polytechnic Institute; A. M. O. Smith, McDonnell-Douglas Corporation; and W. Schönauer, University of Karlsruhe. The methods used and cases treated are indicated in Table 2. All investigators except Smith used an implicit finite-difference method to solve the boundary-layer or viscous shock-layer equations. The numerical methods are described in Refs. 3–6.

Results and Discussion

Case A

The nonequilibrium skin-friction and heat-transfer predictions of Blottner and Smith are within about 5% of each other over the entire body (Fig. 3). Schönauer's equilibrium gas (EQ) prediction of C_{f_∞} is about 10% below, and the perfect gas (γ = 1.4) prediction is about 10% above, these nonequilibrium gas (*NEQ*) results. For St_∞, *EQ* and perfect-gas results are within about 10% of each other and are both about 25% below the *NEQ* results. The *NEQ*, noncatalytic-wall (*NCW*) results of Blottner are not shown, but St_∞ was reduced about 15%. The perfect-gas prediction of St_∞ is therefore within about 10% of the *NEQ*, *NCW* prediction.

From Fig. 4 we see that the predictions of displacement thickness δ^* varied substantially. The *NEQ* values of Blottner are about twice those of Smith, even though their C_{f_∞} and St_∞ predictions are in good agreement, and the *EQ* values of Schönauer are about 25% below Smith's *NEQ* results. The perfect-gas curve is substantially above Blottner's.

A comparison of species profiles at the end of the body (s/r_n = 50) is shown in Fig. 5 from the *NEQ* calculations of Blottner and the *EQ* results of Schönauer. The latter model did not include ionization. Species concentrations near the

Table 2 Test cases computed and methods used

Investigator	JCA	FGB	RTD	AMOS	WS
Gas model					
Binary				A,B	
Multicomponent	B	A,B			A,B
Perfect gas (γ = 1.4)	C		C		
Chemistry					
Frozen				A,B	
Equilibrium				A,B	A,B
Nonequilibrium	B	A,B		A,B	
Numerical method					
Finite difference	*	*	*		*
Differential difference				*	

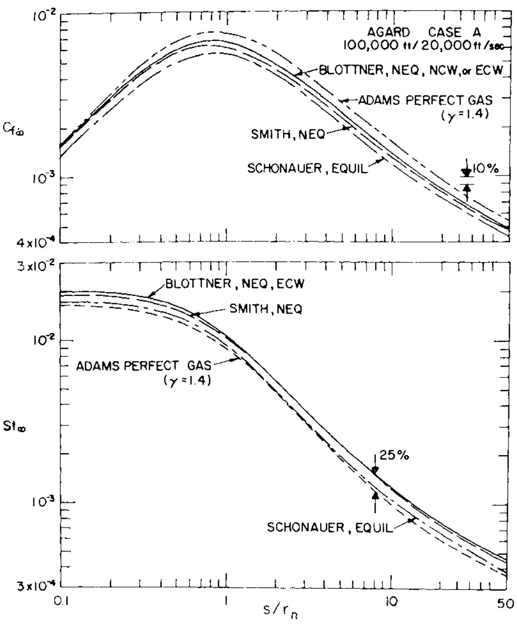

Fig. 3 Skin-friction and heat-transfer distributions for Case A.

wall were in good agreement, and the differences near the outer edge of the boundary layer are probably due mostly to differences in the inviscid boundary conditions from the *EQ* and *NEQ* stream-tube expansions.

The chemical model of Blottner is the most complete and exact, and his data are considered the reference condition for this case. It should also be noted that Adams tried to solve this *NEQ* case and was unable to obtain a convergent solution, since the flow was near equilibrium. Thus, Blottner's ability to solve this case indicates the improvements made in *NEQ, BL* solution methods between 1967 and 1969.

Case B

In Fig. 6 the nonequilibrium skin-friction results of Blottner and Smith are shown as one curve, since the differences were not plottable. Except for the stagnation region ($s/r_n < 1$), all *NEQ* solutions for $C_{f\infty}$ agreed within 5%; Adams' perfect gas prediction was about 60% above his *NEQ* result. For St_∞, the effects of equilibrium catalytic wall (*ECW*) and noncatalytic wall (*NCW*) boundary conditions can be seen. Adams' *ECW* prediction is 25% above his *NCW* results. For $s/r_n > 10$, Blottner's *ECW* is higher (as much as 15%) than Adams' results for the same wall conditions. This will be discussed in more detail below. Adams' perfect gas and

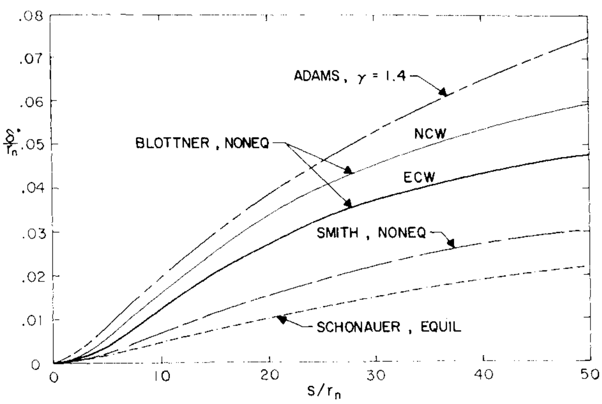

Fig. 4 Boundary-layer displacement-thickness distribution for Case A.

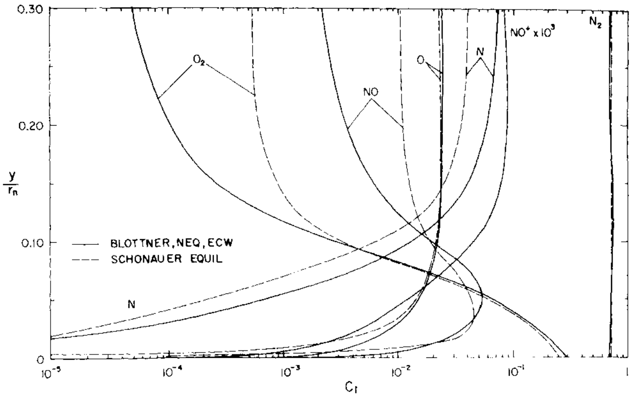

Fig. 5 Species distributions for Case A at $s/r_n = 50$.

NEQ, NCW results are within 5% of each other. Considering all calculations, the *NEQ* heat-transfer predictions differ as much as 50% for $s/r_n > 20$.

The differences in displacement-thickness results (Fig. 7) are even larger. Using Adams' *NEQ, ECW* prediction for reference, Blottner's results for the same chemical model are twice as large, Smith's are 60% higher (but in good agreement with Adams' perfect-gas prediction), and Schönauer's equilibrium results are lower by about 50%.

It is of interest to compare the results of Adams and Blottner, because Adams used the numerical methods developed by Blottner[4] in 1964. Both used 6 species and Blottner and Adams used 7-reaction and 8-reaction models respectively. Adams used Bortner's 1963 reaction-rate coefficients[9] whereas Blottner used Bortner's 1966 data.[10] The differences in the sets of rate data are not expected to affect the $C_{f\infty}$ and St_∞ results significantly. The most significant difference in their methods is that Adams iterated his solution of the conservation equations at each step along the body until u, T, and species profiles differed by less than 0.1% at all points across the boundary layer, while Blottner did not iterate his solution. Their St_∞ predictions (Fig. 6) are identical for $s/r_n < 4$; however, beyond that point differences as large as 20% occur. Also for $s/r_n > 4$, large differences exist in δ^*. Thus, it appears that stepwise iteration is required for accurate results.

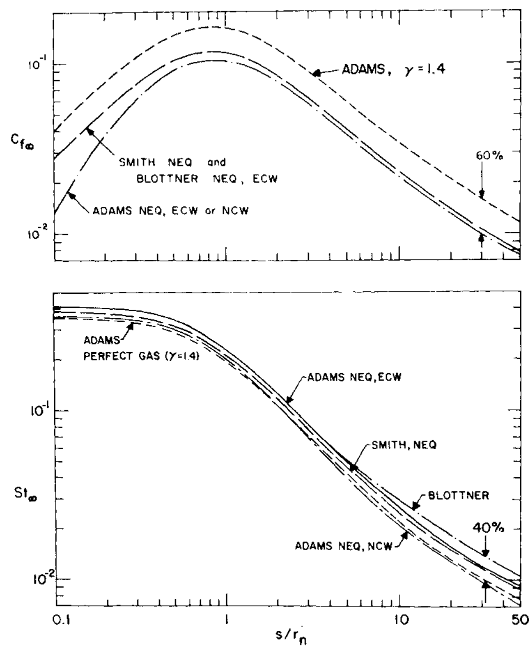

Fig. 6 Skin-friction and heat-transfer distributions for Case B.

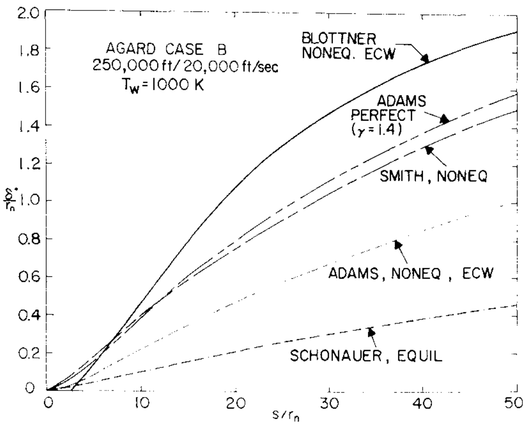

Fig. 7 Boundary-layer displacement-thickness distribution for Case B.

Case C

Figure 8 shows that classical first-order boundary-layer (BL) theory (Adams) underpredicts skin friction by 20–30% over the entire body. Second-order BL theory is within about 10% of the viscous shock-layer result for $s/r_n = 1$ and thereafter increasingly overpredicts $C_{f\infty}$. Whereas the trends of the first-order BL prediction are correct over the entire body, the trends of the second-order theory are incorrect for $s/r_n > 30$, where the effects of vorticity are greatly overpredicted by the second-order theory.

For St_∞, Fig. 8 shows that the first-order theory is within ~10% the viscous shock-layer result over the entire body, whereas again the second-order theory over predicts the viscous shock-layer result by a factor of 2.3 at the end of the body. It is interesting to note that the first-order prediction of St_∞ is in substantially better agreement with the viscous shock-layer results than is the prediction of $C_{f\infty}$. Also, even though higher-order BL (low Re_∞) effects are important, predictions based on classical first-order BL theory are sufficient for predictions of wall heat transfer.

Figure 9 shows that boundary-layer displacement increases the surface pressure by 15–20% relative to the inviscid (Newtonian) curve, over most of the body, whereas the viscous shock-layer results are ~35% higher than the inviscid result. Such differences are large enough to measure, and an experimental test would be most interesting.

Figure 10 presents predicted flowfield variables at the end of the body ($s/r_n = 50$). The inviscid shock-layer results were computed by the author from a perfect-gas ($\gamma = 1.4$), method-of-characteristics (MOC) solution. The first- and second-order boundary-layer results were computed by Adams, and the viscous shock-layer results are from Davis. An additive composite expansion of the (inner) first-order BL results with the (outer) inviscid MOC results can be compared with the viscous shock-layer results. A composite expansion using the second-order BL results was not attempted, since it is clear that second-order theory is not applicable at that location on the body. Also, the composite expansion for the first-order temperature is not shown, since a negative temperature is predicted using the first-order BL result. From Fig. 10, we see that the composite expansion yields a velocity distribution in reasonably good agreement with the viscous shock-layer results; however, agreement with the more complete theory is poor for all other flowfield variables.

Finally, for the conditions of this case, the predictions of boundary-layer theory are substantially in error upon comparison with the viscous shock-layer results. Although the first-order prediction of St_∞ was within 7%, the errors in $C_{f\infty}$ (20–30%) and viscous-induced pressure (35%) predictions were substantial, and the predictions of most flowfield variables were often in error by a factor of two.

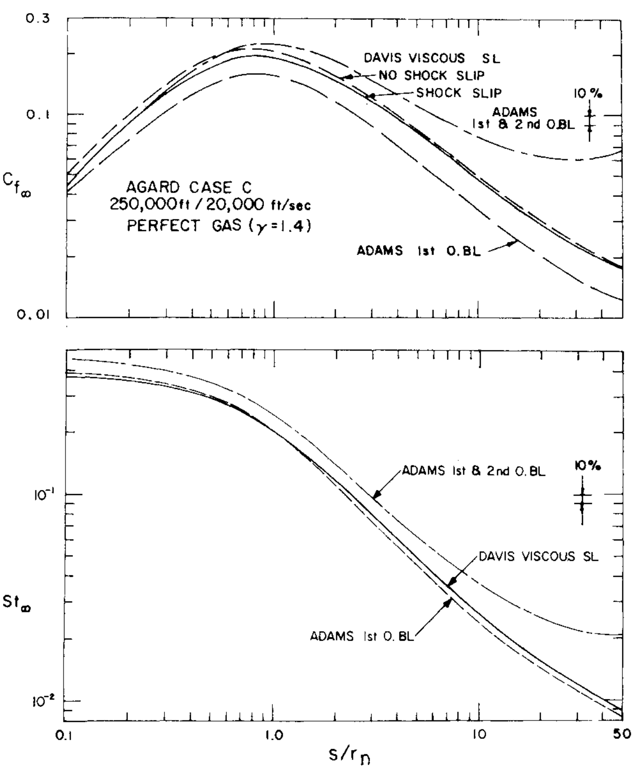

Fig. 8 Skin-friction and heat-transfer distributions for Case C.

Stagnation Point

Stagnation-point velocity, temperature, and species profiles for Case B, multicomponent NEQ, BL, thin viscous shock layer ($TVSL$), and thin viscous shock layer with shock slip ($TVSLSS$) are shown in Fig. 11 for both noncatalytic wall (NCW) and equilibrium catalytic (ECW) wall conditions. The calculations were from Adams. Shock slip reduces the velocity and temperature behind the shock about 20% below the frozen shock-crossing values. The equilibrium inviscid stagnation conditions were used as the outer boundary conditions for the boundary-layer solution.

All species except N_2 are strongly affected by the shock-layer models (Fig. 11c). Including shock slip effects in the TVSL model reduced the concentrations of O, N, and NO by

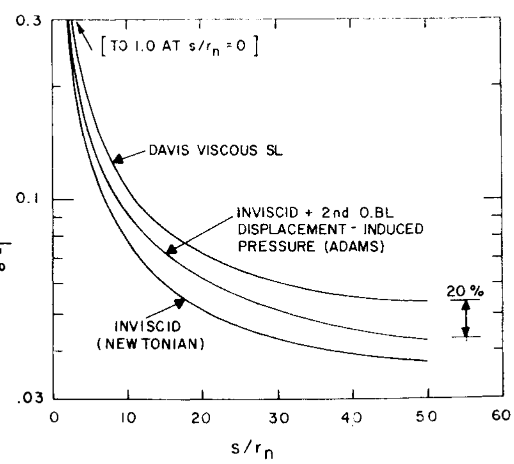

Fig. 9 Surface-pressure distributions for Case C.

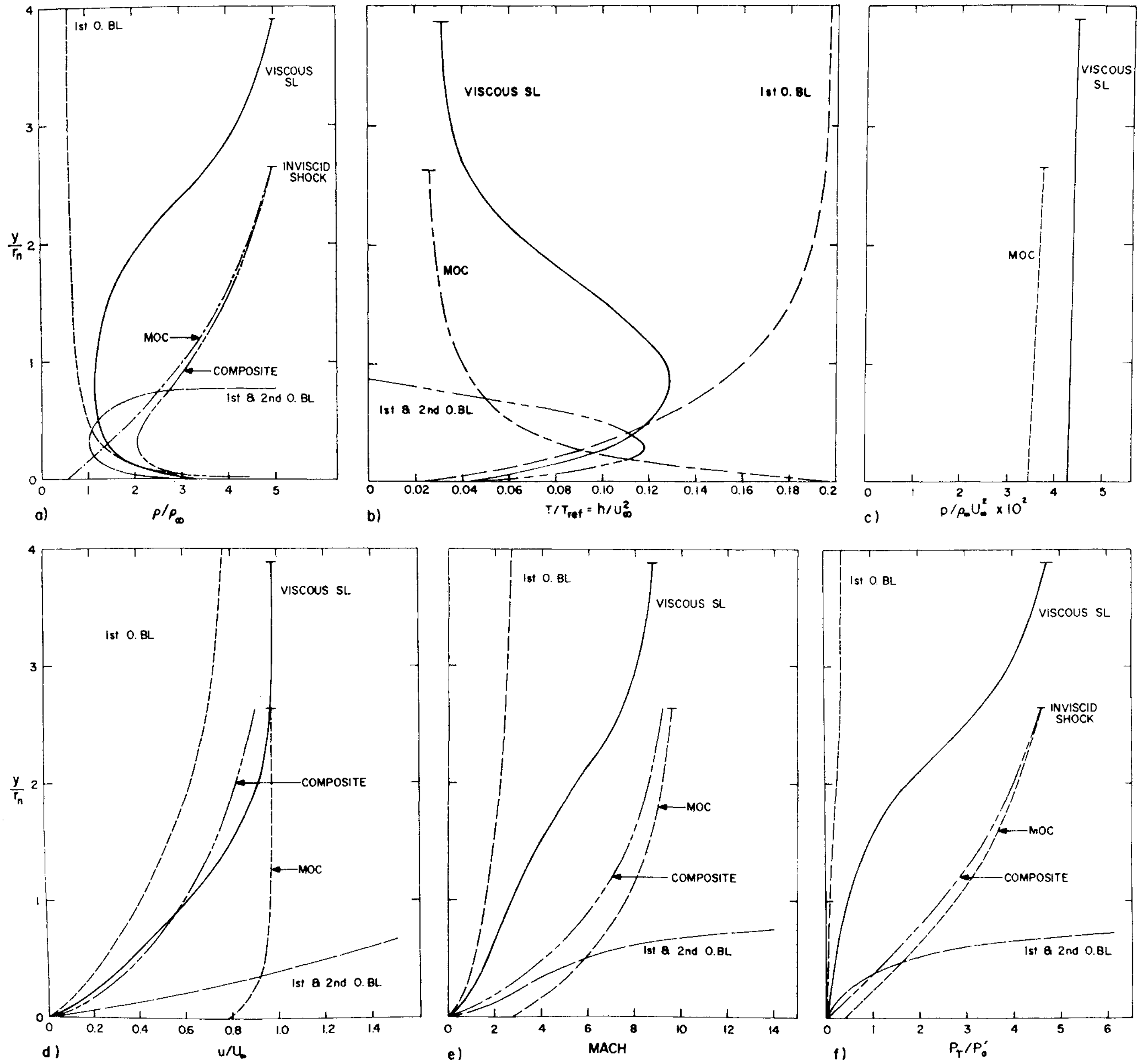

Fig. 10 Shock-layer profiles for Case C at $s/r_n = 50$.

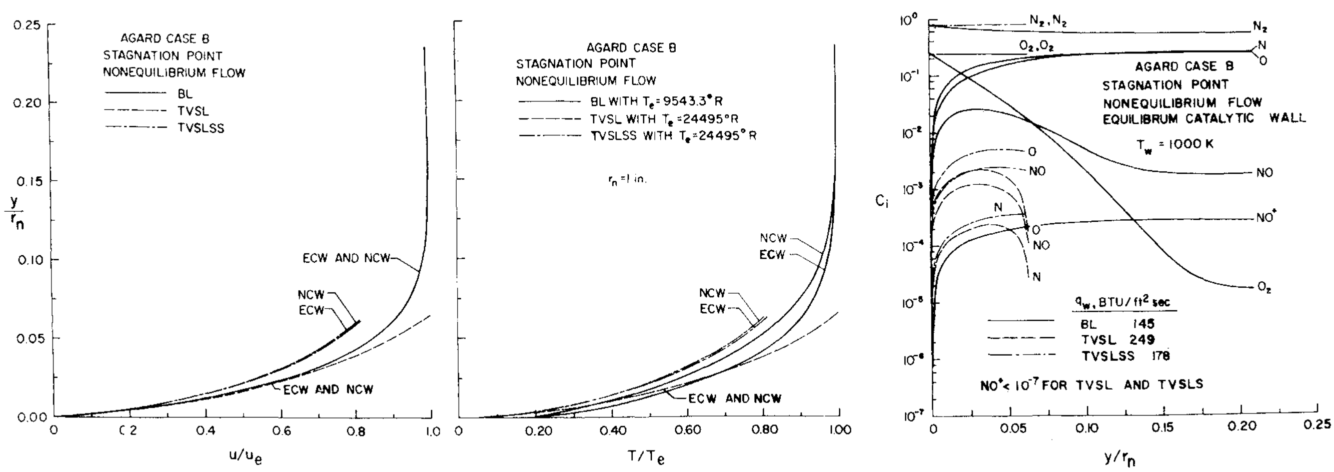

Fig. 11 Stagnation-point profiles for Case B (after Adams).

Table 3 Stagnation-point Stanton numbers

Source	Conditions	A	B	C
Adams	*BL,NEQ,NCW*	...	0.128	...
	BL,NEQ,ECW	...	0.44	...
	TVSL,ECW	...	0.706	...
	TVSL,NCW	...	0.705	...
	TVSLSS,NCW	...	0.52	...
	TVSLSS,ECW	...	0.54	...
	1st *O.BL*	...	...	0.38
	2nd *O.BL*	...	...	0.46
Blottner	*BL,NEQ,NCW*	0.0189	...	...
	BL,NEQ,ECW	0.0204	0.432	...
Davis	*SL*	...	...	0.421
	SLSS	...	...	0.373
Schönauer	*BL,EQ*	0.0177	0.417	...
Smith	*BL,NEQ*	0.0199	0.418	...
	BL,EQ	0.0166	0.354	...
	BL,Frozen	0.0201	0.427	...

about one order of magnitude just behind the shock. The effect could be important if gas radiation were to be considered for these conditions.

Also shown in Fig. 11 (right) for comparison are the predictions of stagnation heat-transfer rate q_w from the three theories. It is not obvious from consideration of the temperature profiles in Fig. 11 (middle) that the viscous shock layer without shock slip should increase q_w by 70%, and including the effects of shock slip should reduce q_w by ~30%. Thus, it is important to consider the effects of transport properties on the shock wave when predicting q_w under similar conditions.

Table 3 compares stagnation-point Stanton number predictions from all available sources and for all conditions considered by the investigators. For Case A the limited data available for *NEQ*, *BL* predictions agree within 5%, and the *EQ*, *BL* predictions agree within about 6%. For Case B, the *NEQ*, BL predictions are within 3%, while the *EQ*, *BL* results differ by 15%.† For the perfect gas ($\gamma = 1.4$) Case C, the first- and second-order predictions were about 10% below and above, respectively, the viscous-shock-layer prediction, and the effects of shock slip reduced *St* by 12%. In comparison, for Case B the effects of shock slip reduced *St* by 23.5%. Therefore, the effects of finite-rate chemistry and shock slip have a stronger influence on the stagnation heat-transfer rate than does shock slip alone in the perfect gas case.

Conclusions

1) Blottner has made substantial improvements in numerical methods for computing viscous flows with finite rate, multicomponent, nonequilibrium chemistry and can compute flowfields near chemical equilibrium.

2) For Case A (100,000 ft), predictions of skin-friction ($C_{f\infty}$) and heat-transfer (St_∞) distributions were within about 15%, of each other whereas displacement thickness (δ^*) differed by a factor of two. Equilibrium and nonequilibrium species profiles at 50 nose radii were controlled primarily by differences in edge conditions from the inviscid streamtube expansion data.

3) For Case B (250,000 ft), nonequilibrium predictions of $C_{f\infty}$ were within 10% of each other while St_∞'s differed by as much as 50% and δ^*'s again differed by a factor of two. Effects of iterating the solution of the conservation equations resulted in differences in heat transfer of 20% using similar numerical methods and chemical data.

4) For Case C (perfect gas, 250,000 ft), first-order boundary-layer predictions of St_∞ were within 10%, whereas predictions of $C_{f\infty}$ were ~30% in error upon comparison with the viscous shock-layer results. Except in the nose region, second-order theory was not applicable, and the viscous shock-layer theory must be used for these conditions. Viscous-to-inviscid surface pressure ratio was about 1.4. Composite expansions of boundary-layer and inviscid (method of characteristics) results did not, in general, yield reliable shock-layer property profiles.

5) For similar chemical and viscous flowfield models, stagnation-point heat-transfer *St* predictions were in good agreement among all investigators. Viscous shock-layer models with nonequilibrium chemistry with and without shock slip substantially affected *St*.

6) Finally, although the ranges of conditions covered by the test cases were not especially broad, substantial differences existed in results from the various prediction methods. Comparison with perfect gas results shows the need for adequate chemical and viscous flowfield models for predicting wall and viscous-layer measurable properties.

† This case is not near chemical equilibrium and these *EQ*, *BL* results are shown only for purposes of comparing numerical results.

References

[1] Lewis, C. H., "Nonreacting and Chemically Reacting Viscous Flows over a Hyperboloid at Hypersonic Conditions," AGARDograph AGARD-AG-147-70, NATO-AGARD, Paris, France, 1970.

[2] Lordi, J. A., Mates, R. E., and Moselle, J. R., "Computer Program for the Numerical Solution of Nonequilibrium Expansions of Reacting Gas Mixtures," Rept. AD-1689-A-6, June 1965, Cornell Aeronautical Lab., Buffalo, N.Y.

[3] Blottner, F. G., "Viscous Shock Layer at the Stagnation Point with Nonequilibrium Air Chemistry," *AIAA Journal*, Vol. 7, No. 12, Dec. 1969, pp. 2281–2288.

[4] Blottner, F. G., "Finite Difference Methods of Solution of the Boundary-Layer Equations," *AIAA Journal*, Vol. 8, No. 2, Feb. 1970, pp. 193–205.

[5] Keltner, G. L., "Laminar Boundary Layer Calculations on Bodies of Revolution in Hypersonic Flow," Rept. DAC-66719, March 1968, McDonnell-Douglas Long Beach, Calif.

[6] Davis, R. T., "The Hypersonic Fully Viscous Shock-Layer Problem," Rept. SC-RR-68-840, Dec. 1968, Sandia, Albuquerque, N. Mex.

[7] Adams, J. C., "Higher-Order Boundary-Layer Effects on Analytic Bodies of Revolution," AEDC-TR-68-57, April 1968, Arnold Engineering Development Center, Tenn.

[8] Blottner, F. G., "Nonequilibrium Laminar Boundary Layer Flow of Ionized Air," *AIAA Journal*, Vol. 2, No. 11, Nov. 1964, pp. 1921–1927.

[9] Bortner, M. H., "Chemical Kinetics in a Re-entry Flowfield," TIS R63SD63, 1963, General Electric.

[10] Bortner, M. H., "Suggested Standard Chemical Kinetics for Flowfield Calculations—A Concensus Opinion," *AMRC Proceedings*, Dept. of Defense, Vol. 14, Pt 1, 1966.